



Fully room temperature and label free biosensing based on an ink-jet printed polymer microdisk laser

ABDUL NASIR,¹ YUYA MIKAMI,¹ RUI YATABE,¹ HIROAKI YOSHIOKA,^{1,*} NILESH VASA,²  AND YUJI OKI¹

¹Graduate School and Faculty of Information Science and Electrical Engineering, Kyushu University, Fukuoka, 819-0395, Japan

²Department of Engineering Design, Indian Institute of Technology Madras, Chennai, 600036, India
**h.yoshioka@ed.kyushu-u.ac.jp*

Abstract: Materials with biomolecule-compatible functional groups are desirable for the fabrication of microdisk lasers used in bio-sensing applications. In this study, a microdisk laser was fabricated using a low-viscosity hyper branched polymer FC-V-50 using ink-jet printing, and was surface-modified at room temperature within a relatively short time compared to conventional methods. The carboxyl functional group of the FC-V-50 polymer was used for surface modification and biotinylation. The adsorption characteristics of the microdisk laser were evaluated using bovine serum albumin, avidin, and streptavidin. This study reports the first demonstration of label-free biosensing using the FC-V-50 polymer-based microdisk laser.

© 2021 Optical Society of America under the terms of the [OSA Open Access Publishing Agreement](#)

1. Introduction

Microcavities have received significant attention for sensing applications owing to their high Q factor, low mode volume, and small size. Among various sensing applications, biosensing applications of microcavities are gaining importance, especially for label free biosensing applications. There are various reports on label free biosensing based on optical sensors [1–5]. Microcavities are also suitable for such applications [6–11] along with other biosensing applications [12–17]. The sensing is based on the shift in resonance wavelength owing to the slight change in the radius of the microcavity or a change in the effective refractive index owing to the adsorption of biomolecules on the surface of the microcavity [6]. Planar microcavities such as microdisks and microrings are suitable for integration on a chip [17,18]. In the case of microdisks, the ink-jet printing technique can be used for fully room-temperature, on-site, and on-demand fabrication. Our group previously demonstrated the fabrication of microdisk lasers using an ink-jet printing method [19], which allows the fabrication of microdisks with less wastage of materials compared to conventional methods [11]. There have been various reports on biosensing using active and passive microdisks. In the case of passive microdisks, evanescent wave-based coupling methods are used to couple tunable laser diodes to the microdisk [10]. By contrast, free-space optics can be used for the excitation of an active microdisk doped with the gain medium, and owing to on-chip lasing, a high sensitivity can be achieved [11].

A wide variety of materials such as polymers and silica [10–14] have been used in the past for the fabrication of microdisks for biosensing applications. Most biosensing applications are based on an avidin-biotin interaction owing to their high sensitivity and selectivity. The interaction between avidin and biotin is the strongest known non-covalent interaction and has been used for the development of various biosensing systems [20]. To use microdisks for avidin-biotin based biosensing, biotinylation is needed to covalently attach biotin to the microdisk surface. This can be achieved by attaching a functional group that is compatible with the covalent binding of biotin onto the microdisk surface through a surface modification. Therefore, the surface modification of

the microdisks is an important aspect in avidin-biotin-based biosensing. The strategy for surface modification depends on the nature of the material. In the case of silica-based microcavities, the microcavity surface was oxidized using high-temperature treatments at 50°C to expose hydroxyl functional groups on the microcavity surface. Further, it was treated with aminopropyl triethoxysilane (APTES) to attach amine functional groups onto the surface [9]. In another study, an amine-reactive pentafluoro phenyl ester was attached to a polymethyl methacrylate (PMMA) polymer-based microdisk laser fabricated using a lithography method [11]. In this case, a pentafluoro phenyl ester was attached to the microdisk surface through chemical vapor deposition. This is a multi-step process that involves the sublimation of the pentafluoro phenyl precursor at 120°C, pyrolysis at 560°C, and deposition on the microdisk at 15°C. Therefore, the procedure for surface modification is a tedious and time-consuming process that often involves high-temperature treatments of microcavities. These methods cannot be used for all types of materials, particularly in the case of polymer-based microcavities that cannot withstand high temperatures.

In this study, a newly developed low-viscosity hyper branched polymer FC-V-50, which is characterized by a hydrophilic carboxyl functional group and a chain of fluorinated functional group CF_2 which is hydrophobic, was used for the fabrication of microdisk lasers by ink-jet printing method. Since the ink-jet printing requires low viscosity ink for the stable ejection of droplets from the nozzle, the low viscosity of the hyper branched polymer compared to polymers like PMMA or Polyvinyl alcohol (PVA) is highly advantageous for ink-jet printing [21,22]. Therefore, by using the low viscosity hyper branched polymer FC-V-50, the on-site and on-demand fabrication of FC-V-50 based microdisk lasers can be carried out by ink-jet printing at room temperature in a short time. The lasing action of FC-V-50 based microdisk laser was reported previously [23]. Once the ink droplet from nozzle is deposited on fluorinated ethylene propylene (FEP) substrate, the evaporation of solvent causes Marangoni convection and distribution of FC-V-50 polymer in the form of a disk and its solidification. In addition, the carboxyl functional group of FC-V-50 polymer eliminates the need for covalently attaching a functional group to the microdisk surface by using high-temperature treatment. Also, this method permits the fabrication of microdisks on all types of substrates at room temperature. Therefore, the use of FC-V-50 polymer for biosensing applications allows the onsite and on demand fabrication and biotinylation of microdisks at room temperature within a relatively short time compared to the conventional method [11]. Because the polymer has low viscosity, it can also be used for other applications such as spin coating [24]. This study reports the first biosensing demonstration using the FC-V-50 polymer-based microdisk laser conducted entirely at room temperature. In this study, the physical adsorption characteristics of bovine serum albumin (BSA) and avidin on non-biotinylated microdisk surfaces were evaluated. In addition, factors affecting the non-specific adsorption of proteins on microdisk surfaces, such as hydrophobicity and surface charge, were studied. Subsequently, label-free detection of avidin and streptavidin using biotinylated microdisks was conducted. For this, biotinylation was carried out using the carboxyl functional group of the FC-V-50 polymer at room temperature. Because the biotinylation and fabrication of microdisks were carried out at room temperature, the use of FC-V-50 polymer allows the on-site and on-demand fabrication of microdisk laser-based biosensors. Biotinylated microdisks along with avidin can be used for the detection of antigen-antibody interactions in the future.

2. Experimental methods

To evaluate the optical characteristics of the FC-V-50 polymer, the absorption spectrum and refractive index were measured. In this case, 10 wt.% of FC-V-50 in ethanol was used for evaluating the absorption characteristic by using a spectrophotometer (JASCO, V-630). The refractive index of the FC-V-50 polymer was evaluated using a spectroscopic ellipsometry

analyzer (Semilab, SE-2000). For this, the FC-V-50 polymer was spin-coated on a PMMA substrate.

To determine the suitability of the FC-V-50 polymer for biosensing applications, the physical characteristics of the polymer, such as the zeta potential and hydrophobicity, which can cause the non-specific adsorption of biomolecules on the polymer, were measured. The zeta potential of the polymer was measured using an electro-kinetic analyzer (Anton Paar, GmbH, SurPASS). For this, the FC-V-50 polymer was spin-coated on a PMMA substrate and used for the measurements. The zeta potential of the polymer was measured at different pH values in potassium chloride (KCl) solution. To measure the hydrophobicity, a contact angle meter (Kyowa, DM-500) was used. The sample was prepared by spin coating the FC-V-50 polymer on a PMMA film.

Figure 1 shows the schematic of the microdisk fabrication and biotinylation for the label-free detection of avidin. The FC-V-50 polymer (refractive index of 1.53) based microdisk was fabricated on FEP, which has a refractive index of 1.35, using the ink-jet printing method. In this case, a 20 wt.% FC-V-50 polymer in a mixture of ethanol and cyclohexanone (1:1 volume ratio) doped with pyrromethene597 (concentration of 8 mM) was used as ink for the fabrication of microdisk lasers. A high-accuracy manipulation robot (Musashi Engineering, Inc., SHOT mini 200Ω) with a 40-μm diameter piezo electric nozzle (Cluster Technology Co. Ltd., PIJ-40ASET) was used for the fabrication of the microdisk laser. For the ejection of stable ink droplets, the piezoelectric nozzle voltage and frequency were optimized at 5.1 V and 37 Hz, respectively. In addition, a meniscus suction pressure of −0.2 kPa was applied at the nozzle opening.

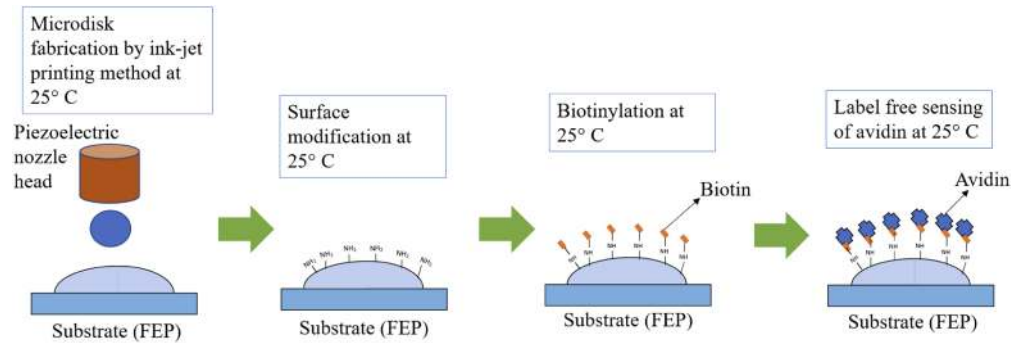


Fig. 1. Schematic of microdisk fabrication and biosensing.

To immobilize biotin on the microdisk surface, the surface of the microdisk was modified by covalently attaching amine functional groups using 1-ethyl-3-(3-dimethylaminopropyl) carbodiimide (EDC) and N-hydroxysuccinimide (NHS) reagents at 25 °C [25], as shown in Fig. 1. The modification of the microdisk surface was realized using the carboxyl functional group of the FC-V-50 polymer. For the covalent binding of amine functional groups, the carboxyl functional group in FC-V-50 was activated by incubating the microdisk in a solution of EDC (0.4 M) and NHS (0.1 M) in water for 1 h. The activation of the carboxyl functional group was followed by covalent binding of the amine functional group, which was achieved by incubating the microdisk in a solution of ethylenediamine (0.1 M) in borate buffered saline (BBS) for 30 min. For the biotinylation of the microdisks, the surface-modified microdisks were immersed in a solution of 10 ppm sulfo-nhs-biotin in phosphate buffered saline (PBS) for 10 min. After biotinylation, the microdisks were immersed in ethanolamine-HCl for 1 h to deactivate the unreacted NHS esters. Once the biotinylation of the microdisk was accomplished, it was used for the label-free detection of avidin. All protein solutions used in the experiments were prepared by mixing proteins in phosphate buffered saline (PBS) solution. Biotinylation was also carried out by incubating the microdisk in biotin-PEG11-amine of 10 ppm for 30 min. The biotin-PEG11-amine has longer

spacer arm compared to sulfo-nhs-biotin and hence improves the interaction with avidin. The microdisks were first incubated in EDC and NHS for 30 min. After biotinylation, the microdisk was incubated in a BBS buffer for 30 min to deactivate the unreacted NHS esters. Biotinylated microdisks were then used for the label-free detection of streptavidin.

Figure 2 shows a schematic of the experimental setup used for the microdisk laser-based biosensing. The microdisk was excited using a frequency-doubled Nd:YAG laser (Quantas Q1D, Q1D-SH/TH/FH-1064) at a wavelength of 532 nm and at a pulse repetition rate of 10 Hz with pulse width of 8 ns. A plano-concave lens ($f = 2$ cm) was used to focus the laser beam on the microdisk. After blocking the beam at 532 nm using a long pass filter, the whispering gallery mode (WGM) signal was collected with an optical microscope at a magnification of 100 \times . The WGM signal was coupled to the spectrometer (SOLAR TII, MS7504) which had a slit width of 0.1 mm and an exposure time of 2 s by using an optical fiber (Thorlabs, Inc., AFS105/125Y). The resolution of the spectrometer was 0.025 nm. An FEP substrate with a microdisk was attached to the PMMA substrate using a silica seal to avoid bending.

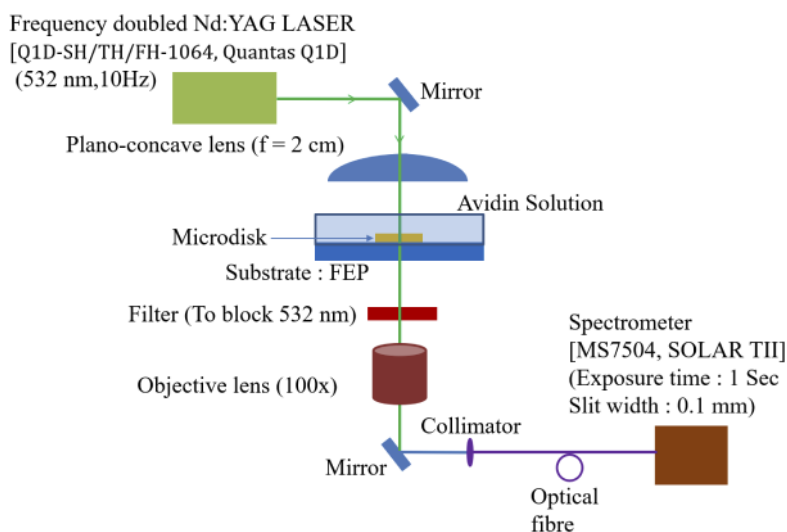


Fig. 2. Experimental setup for the microdisk laser based biosensing.

3. Results and discussions

3.1. Characteristics of FC-V-50 hyperbranched polymer

Figure 3 shows the optical properties of the FC-V-50 polymer, which include the absorption spectrum and refractive index. Figure 3(a) shows the absorption spectrum of the FC-V-50 polymer. The polymer has a low absorption within the visible and infra-red regions. Therefore, the FC-V-50 polymer can be doped with a fluorescent dye within the visible region. Figure 3(b) shows the refractive index of the FC-V-50 polymer. Because the refractive index of the polymer is 1.53 at 633 nm, the FC-V-50 polymer-based microdisk can be fabricated on substrates such as FEP (refractive index of 1.35). The refractive index of the FC-V-50 is 1.55 at 590 nm. In the case of avidin solution of 5 ppm concentration, the refractive index is 1.33 at 590 nm based on the specific refractive increment value [26].

The zeta potential of the polymer was measured at different pH values by using an electrokinetic analyzer, as shown in Fig. 4(a). The zeta potential was zero at pH 3.8, which indicates the presence of carboxyl functional groups. At pH 7.4, the zeta potential was -48 mV; hence,

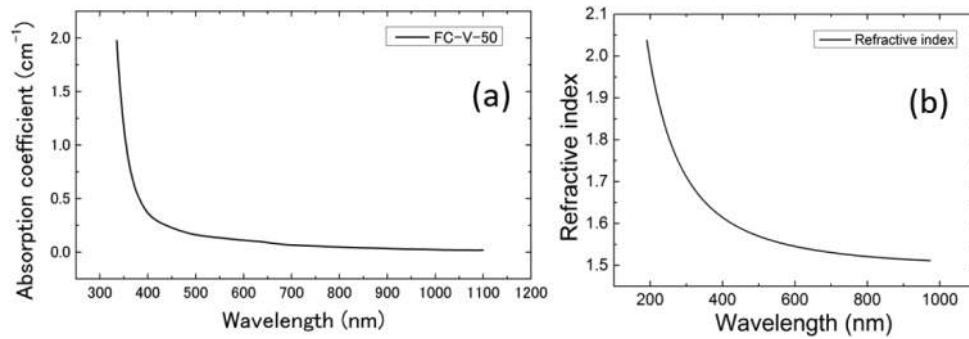


Fig. 3. (a) Absorption spectrum and (b) refractive index profile of FC-V-50 polymer.

the polymer was negatively charged. This indicates the possibility of non-specific adsorption of positively charged biomolecules when the polymer is used for biosensing applications.

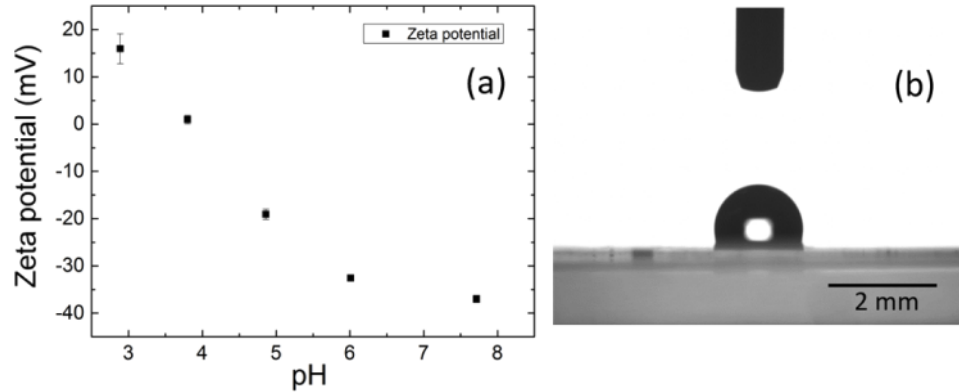


Fig. 4. (a) Zeta potential and (b) contact angle of FC-V-50 polymer.

The contact angle of the FC-V-50 polymer was measured as 110° , as shown in Fig. 4(b) and this indicates that the polymer is hydrophobic. This is due to the presence of fluorinated functional group CF_2 which results in low surface tension hence hydrophobic [27]. The presence of CF_2 also results low refractive index of FC-V-50 due to the low polarizability of fluorine [28]. Therefore, the non-specific adsorption of biomolecules owing to hydrophobic interactions can be expected when the polymer is used for biosensing applications. However, the hydrophobicity of the polymer ensures stability in water.

3.2. Ink-jet printing of the microdisk laser

The FC-V-50 microdisk was fabricated on an FEP substrate using the ink-jet printing method. Once the microdisk laser was fabricated, the diameter of the microdisk laser was estimated to be $70\ \mu\text{m}$ by using an optical microscope (Nikon, ECLIPSETE2000-U), as shown in Fig. 5(a). In addition, the edge angle of the microdisk was measured as 15.8° using atomic force microscopy (AFM) (Keyence Corp, VN-8000), as shown in Fig. 5(b). A low edge angle is advantageous for sensing applications because it reduces the confinement of WGM and increases the interaction of the WGM with the analyte, as reported in a previous study [29].

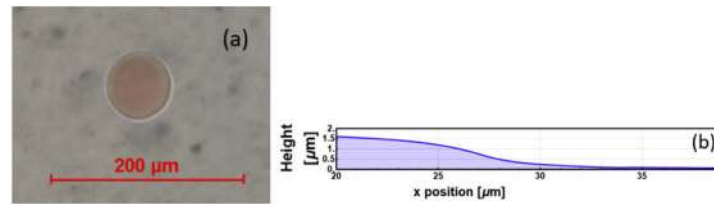


Fig. 5. (a) Optical microscopic image of microdisk and (b) edge profile of microdisk

3.3. Biosensing using the FC-V-50 based microdisk laser

For biosensing applications, the stability of FC-V-50 microdisks in water is an important aspect. To confirm this, FC-V-50 based microdisks were immersed in PBS solution for 15 min. No cracks were observed on the microdisk edge after incubation in PBS, as shown in Fig. 6. Also, the contact angle measurement of FC-V-50 as shown in Fig. 4(b) shows that the polymer is hydrophobic. This reveals that the microdisk is stable in liquid environment and therefore suitable for biosensing applications.

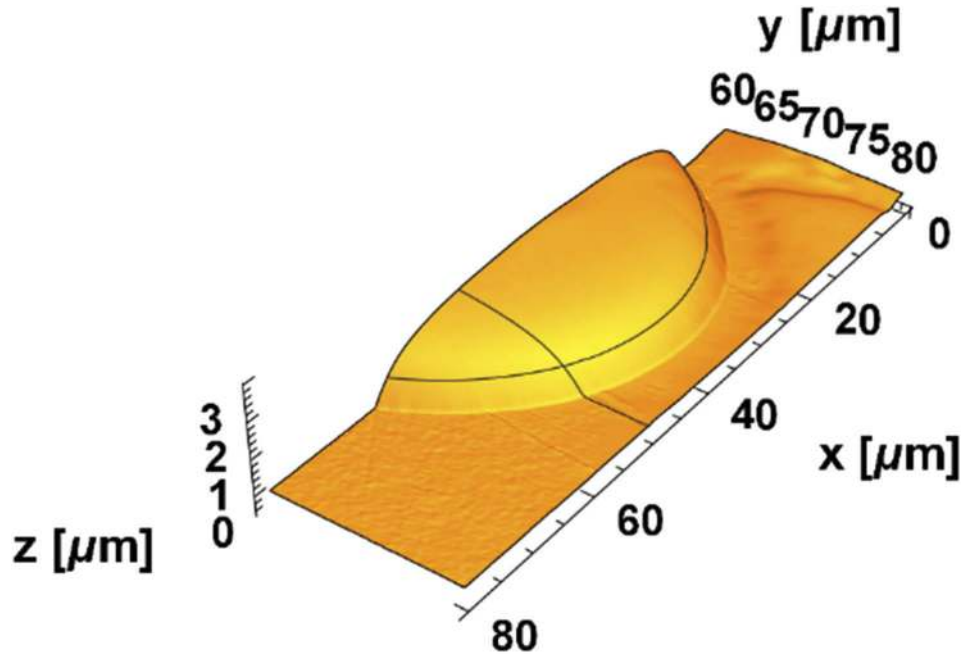


Fig. 6. AFM image of microdisk edge after incubating in water for 15 min.

Biosensing using the FC-V-50 polymer based microdisk laser was carried out by monitoring the adsorption of proteins on the microdisk surface. In order to monitor the adsorption of protein on microdisk surface, the microdisks were immersed in PBS solution for 10 min, and the WGM spectra were recorded three times before immersion in protein solution. Because the microdisks were immersed in PBS solution, the mode shift is only due to dye degradation. By contrast, mode shifts in protein mixed PBS solution are due to dye degradation and protein adsorption. Therefore, mode shifts in PBS solution were used to obtain a reference to measure the mode shift owing to protein adsorption. Also, from the lasing characteristics of FC-V-50 microdisk laser [23], it was found that the mode intervals are same when the microdisk excited with different

energy densities. This indicates that there is no refractive index modulation due to pump power density. After exposing the microdisks to the protein solution, they were again immersed in PBS solution, and the mode shifts were measured to confirm the adsorption of protein on the microdisk surface. A slide glass was attached to the microdisk after dropping a droplet of analyte onto the microdisk to obtain a uniform distribution of analyte on the microdisk surface.

To study the interaction between the polymer used to fabricate the microdisk and proteins, the physical adsorption characteristics of a non-biotinylated microdisk were evaluated. First, the adsorption characteristics of the microdisk laser were evaluated using 100 ppm of BSA in PBS solution, and WGM spectra were recorded at different time intervals. Figure 7(a) shows the WGM spectrum of the microdisk in PBS with wavelength ranging from 576.86 nm to 603.70 nm as shown in the x-axis. The temporal variation of the mode shifts owing to BSA adsorption is shown in Fig. 7(b) for different intervals of time as shown in the x-axis. The microdisk was incubated in BSA solution for 25 min. and then it was rinsed using PBS and again incubated in PBS till 40 min. to confirm the adsorption of BSA on the microdisk surface. The blue shift in the WGM mode indicates that the adsorption of BSA on the microdisk surface causes a decrease in the effective refractive index. Once the microdisk was exposed to the BSA solution, it was again immersed in a PBS solution and mode shifts were again measured. The red shift in the spectrum in PBS, as shown in Fig. 7(b), indicates that BSA is not completely washed off from the microdisk surface.

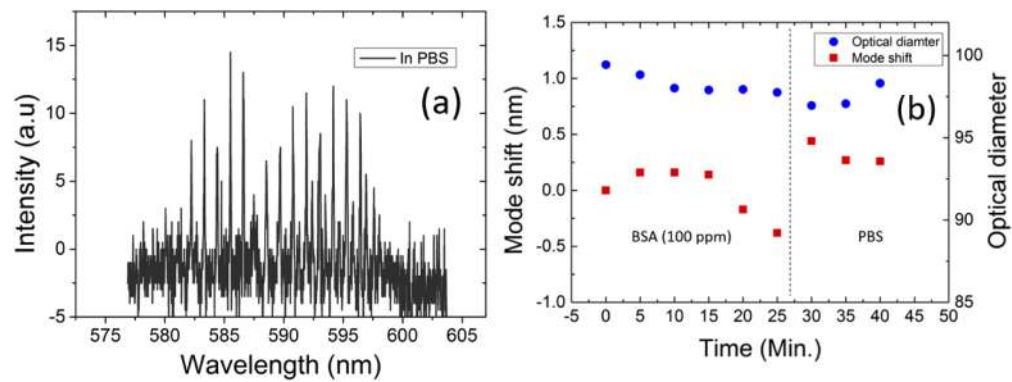


Fig. 7. (a) WGM spectra of microdisk laser in PBS and (b) changes in WGM mode in BSA and PBS solutions.

The decrease in effective refractive index could be due to the formation of multiple layers of BSA on the microdisk surface. To confirm the decrease in the effective refractive index, the optical diameter of the microdisk was calculated from free spectral range (FSR) based on the following equation:

$$\Delta\lambda = \frac{\lambda^2}{2\pi nR} \quad (1)$$

where $\Delta\lambda$ is the FSR, λ is the central wavelength, n is the effective refractive index, and R is the radius of the microdisk.

$$OD = \frac{\lambda^2}{\pi\Delta\lambda} \quad (2)$$

The optical diameter (OD) of the microdisk is defined in (2) and was calculated as shown in Fig. 7(b). The decrease in optical diameter indicates that the effective refractive index decreases owing to the formation of multiple layers of BSA.

Figure 8(a) and Fig. 8(b) show the temporal variation of mode shift owing to the adsorption of 5 ppm avidin on non-biotinylated microdisks and biotinylated microdisks for different intervals

of time as shown in the x-axis of Fig. 8(a) and Fig. 8(b). The microdisks were incubated in avidin solution of 5 ppm for 8 min. and WGM spectra were recorded for every 2 min. and then microdisks were rinsed using PBS and again incubated in PBS till 14 min. to confirm the adsorption of avidin on the microdisk surface. Once the reference was obtained by immersing the non-biotinylated microdisk in PBS solution, the microdisk was then immersed in an avidin solution of 5 ppm concentration, and the spectra were recorded at different time intervals. As time progressed, a blue shift in WGM in the spectra was observed for non-biotinylated microdisks, as shown in Fig. 8(a). This indicates that physical adsorption results in the formation of multiple layers of avidin on the microdisk surface. The decrease in optical diameter reveals that this causes a decrease in the effective refractive index and hence a blue shift in the spectrum. In the case of the biotinylated microdisk, a red shift was observed in the spectrum, as shown in Fig. 8(b). This indicates that the chemical adsorption of avidin on the microdisk surface results in the formation of a monolayer of avidin-biotin complex, and the red shift in the spectrum reveals that this causes an increase in the effective refractive index. After washing and immersing the microdisks in PBS solutions, both biotinylated and non-biotinylated microdisks showed red shifts in the WGM modes. This indicates that an excess amount of avidin was removed from the microdisk surface. The optical diameter after washing was less for biotinylated microdisk, indicating an avidin-biotin interaction.

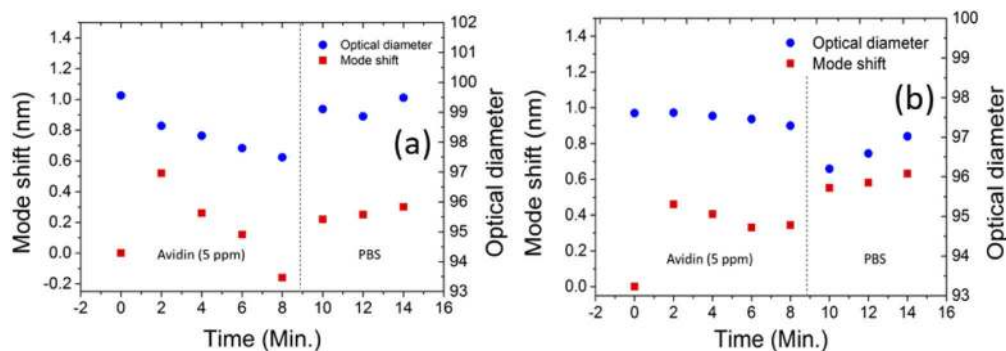


Fig. 8. Mode shift due to avidin adsorption on (a) non-biotinylated microdisk and (b) biotinylated microdisk.

The surface of the FC-V-50 based microdisk is hydrophobic, which could lead to the non-specific adsorption of biomolecules. When biomolecules adsorb on the microdisk surface, they form multiple layers with first layer on the microdisk and covers most of the area of the microdisk surface. This results in a weak adsorption of the successive layers and the penetration of PBS between layers. Because of this, the successive layers become less dense than the first layer and have low refractive indices compared to the first layer. This is in good agreement with a previously reported work in which the adsorption of proteins on hydrophobic and hydrophilic surfaces were studied [30]. In the case of evanescent wave-based sensors such as microdisk, more contrast in refractive index between analyte solution and waveguide is desirable [1,2]. This avoids the interaction of evanescent field with bulk solution and improve the sensitivity of the device for the detection of biomolecules adsorbed on the surface of the sensor. In the case of FC-V-50 based microdisk, the refractive index of the microdisk is 1.55 and that of analyte solution is approximately 1.33. This results in longer evanescent field penetration depth and the evanescent field interact with the bulk solution. From the finite element method (FEM) simulation of microdisk based on Oxborrow model [31], the evanescent field penetration depth was estimated as 189 nm. However, the thickness of the first layer of avidin adsorbed on the microdisk is approximately equal to the size of the avidin which is 6 nm if 100% surface coverage

is assumed. Since the evanescent field depth is 189 nm it interacts with the first layer as well as the successive layers. Because the refractive index of the successive layer is decreasing the mode shift is also decreasing as shown in Fig. 7(b) and Fig. 8(a) for the adsorption of BSA and avidin on non-biotinylated microdisks. In the case of avidin biotin interaction, the first layer is thicker than that the previous case and this results less decrease in mode shift as shown in Fig. 8(b).

Therefore, biotinylated microdisk lasers can be used for label-free detection of avidin. However, non-specific adsorption can occur owing to hydrophobic and electrostatic interactions between the microdisk surface and avidin. The isoelectric point of avidin is 10.5; hence, it has a positive charge at pH 7.4. This results in electrostatic interactions between avidin and the negatively charged FC-V-50 microdisk surface. Therefore, it is important to minimize the non-specific adsorption of avidin on the microdisk surface owing to hydrophobic and electrostatic interactions between avidin and microdisk surfaces for realizing microdisk laser-based label-free biosensors with high sensitivity and selectivity.

Various attempts have been made to minimize the non-specific adsorption of biomolecules on biosensor surfaces owing to hydrophobic and electrostatic interactions [32–35]. Most of these methods require a tedious modification of the biosensor surface. However, BSA blocking is a simple and efficient method to minimize non-specific adsorption owing to hydrophobic interactions [35]. To make the microdisk surface hydrophilic to prevent non-specific adsorption, BSA blocking was carried out using a 1wt./v% BSA solution in PBS. For this, microdisks after biotinylation were incubated in a 1wt./v% BSA solution for 30 min. Biotinylation was carried out by incubating the microdisk for 30 min in 10 ppm of biotin-PEG11-amine after incubation in EDC and NHS for 30 min. To avoid non-specific adsorption owing to electrostatic interactions, streptavidin was used for label-free biosensing. The isoelectric point of streptavidin is 5, and hence, it has a negative charge at pH 7.4. To avoid further exposure of hydrophobic sites during the adsorption of streptavidin, 1000 ppm of BSA in PBS was used for the preparation of streptavidin solutions. Once the reference was measured by incubating biotinylated microdisks in 1000 ppm of a BSA solution, they were used for the label-free detection of streptavidin of different concentrations, as shown in Fig. 9. The biotinylated microdisks were incubated in streptavidin solutions of different concentrations and mode shift was measured at different intervals of time as shown in the x-axis of Fig. 9. The mode shift measurement started at 0 min and continued for different intervals of time as shown in Fig. 9. The maximum mode shifts obtained for 5 ppm,

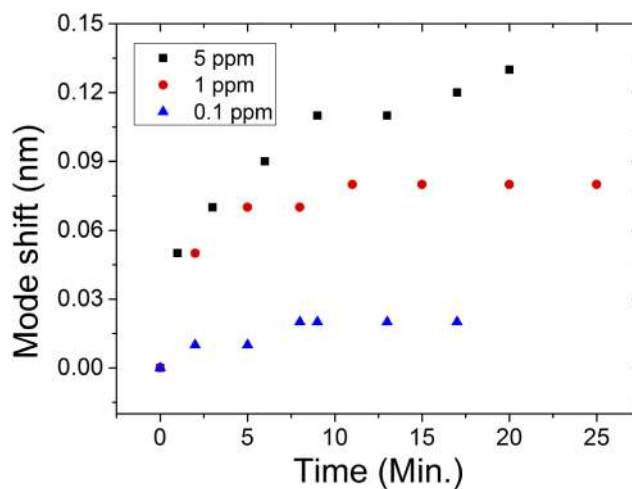


Fig. 9. Mode shift owing to the adsorption of different concentrations of streptavidin on biotinylated microdisks.

1 ppm, and 0.1 ppm of streptavidin are 0.13, 0.8, and 0.02 nm, respectively. In the case of BSA blocked microdisk used for the label free detection of streptavidin, very thick layer of BSA was formed on the microdisk due to high concentration of BSA used for blocking. As a result, a small portion of evanescent wave interacts with analyte solution containing streptavidin. This result low mode shift compared to the adsorption of avidin on biotinylated microdisk without BSA blocking. The maximum mode shift observed in the case of BSA blocked microdisk is 0.13 nm as shown in Fig. 9. On the other hand, maximum mode shift observed in the case of biotinylated microdisk without BSA blocking was 0.48 nm when incubated in avidin solution of 5 ppm as shown in Fig. 8(b).

4. Conclusions

A hyper-branched polymer FC-V-50 based microdisk laser was fabricated using ink-jet printing and biotinylated at room temperature. The zeta potential of the polymer was estimated to be -48 mV at pH 7.4, indicating that the microdisk surface is negatively charged. The contact angle of the polymer was measured as 110° , and hence the polymer was hydrophobic, and this ensures stability in water. In the case of non-biotinylated microdisks, a multilayer formation owing to a non-specific adsorption of BSA and avidin was observed. By contrast, the adsorption of avidin on biotinylated microdisks formed a monolayer of avidin-biotin complex and caused a red shift in the spectrum but there was non-specific adsorption due to hydrophobic interactions. To completely eliminate non-specific protein adsorption, BSA blocking of the biotinylated microdisk was carried out to make the microdisk surface hydrophilic, and negatively charged streptavidin was used to avoid electrostatic interactions. Subsequently, label-free detection of streptavidin at different concentrations was demonstrated. Because the fabrication and biotinylation of FC-V-50 polymer-based microdisk lasers can be carried out entirely at room temperature and on-site, such devices have an immense potential as a label-free biosensor for various biosensing applications.

Funding. Core Research for Evolutional Science and Technology (JPMJCR20T4); Japan Society of Applied Physics (JP18K14149, JP19KK0379, JP20J12903).

Acknowledgements. The authors would like to thank Nissan Chemical Corporation (Planning & Development Department, Performance Materials Division) for providing the fluorinated hyperbranched polymer used in this study.

Disclosures. The authors declare no conflicts of interest.

References

1. M. Lu, S. S. Choi, U. Irfan, and B. T. Cunningham, "Plastic distributed feedback laser biosensor," *Appl. Phys. Lett.* **93**(11), 111113 (2008).
2. E. Heydari, J. Buller, E. Wischerhoff, A. Laschewsky, S. Döring, and J. Stumpe, "Label-free biosensor based on an all-polymer DFB laser," *Adv. Opt. Mater.* **2**(2), 137–141 (2014).
3. A. Retolaza, J. M. Perdiguero, S. Merino, M. M. Vidal, P. G. Boj, J. A. Quintana, J. M. Villalvilla, and M. A. D. García, "Organic distributed feedback laser for label-free biosensing of ErbB2 protein biomarker," *Sens. Actuators, B* **223**, 261–265 (2016).
4. K. Watanabe, M. Nomoto, F. Nakamura, S. Hachuda, A. Sakata, T. Watanabe, Y. Goshima, and T. Baba, "Label-free and spectral-analysis-free detection of neuropsychiatric disease biomarkers using an ion-sensitive GaInAsP nanolaser biosensor," *Biosens. Bioelectron.* **117**, 161–167 (2018).
5. X. Shi, K. Ge, J. H. Tong, and T. Zhai, "Low-cost biosensors based on a plasmonic random laser on fiber facet," *Opt. Express* **28**(8), 12233–12242 (2020).
6. F. Vollmer and S. Arnold, "Whispering gallery mode biosensing: label free detection down to single molecules," *Nat. Methods* **5**(7), 591–596 (2008).
7. A. Ramachandran, S. Wang, J. Clarke, S. J. Ja, D. Goad, L. Wald, E. M. Flood, E. Knobbe, J. V. Hryniewicz, S. T. Chu, D. Gill, W. Chen, O. King, and B. E. Little, "A universal biosensing platform based on optical micro-ring resonators," *Biosens. Bioelectron.* **23**(7), 939–944 (2008).
8. X. Li, Z. Zhang, S. Qin, T. Wang, F. Liu, M. Qiu, and Y. Su, "Sensitive label-free and compact biosensor based on concentric silicon-on-insulator microring resonators," *Appl. Opt.* **48**(25), F90–94 (2009).
9. K. D. Vos, I. Bartolozzi, E. Schacht, P. Bienstman, and R. Baets, "Silicon-on-Insulator microring resonator for sensitive and label-free biosensing," *Opt. Express* **15**(12), 7610–7615 (2007).

10. S. M. Grist, S. A. Schmidt, J. Flueckiger, V. Donzella, W. Shi, S. T. Fard, J. T. Kirk, D. M. Ratner, K. C. Cheung, and L. Chrostowski, "Silicon photonic micro-disk resonators for label-free biosensing," *Opt. Express* **21**(7), 7994–8006 (2013).
11. S. F. Wondimu, M. Hippler, C. Hussal, A. Hofmann, S. Krammer, J. Lahann, H. Kalt, W. Freude, and C. Koos, "Robust label-free biosensing using microdisk laser arrays with on-chip references," *Opt. Express* **26**(3), 3161–3173 (2018).
12. H. Ghali, P. Bianucci, and Y. Peter, "Wavelength shift in a whispering gallery microdisk due to bacterial sensing: a theoretical approach," *Sens. Biosensing Res* **13**, 9–16 (2017).
13. M. Eryürek, Z. Tasdemir, Y. Karadag, S. Anand, N. Kilinc, B. E. Alaca, and A. Kiraz, "Integrated humidity sensor based on SU-8 polymer microdisk microresonator," *Sens. Actuators, B* **242**, 1115–1120 (2017).
14. R. W. Boyd and J. E. Heebner, "Sensitive disk resonator photonic biosensor," *Appl. Opt.* **40**(31), 5742–5747 (2001).
15. S. Arnold, M. Khoshima, I. Teraoka, S. Holler, and F. Vollmer, "Shift of whispering-gallery modes in microspheres by protein adsorption," *Opt. Lett.* **28**(4), 272–274 (2003).
16. F. Vollmer, S. Arnold, D. Braun, I. Teraoka, and A. Libchaber, "Multiplexed DNA quantification by spectroscopic shift of two microsphere cavities," *Biophys. J.* **85**(3), 1974–1979 (2003).
17. D. Kim, P. Popescu, M. Harfouche, J. Sendowski, M. E. Dimotsantou, R. C. Flagan, and A. Yariv, "On-chip integrated differential optical microring refractive index sensing platform based on a laminar flow scheme," *Opt. Lett.* **40**(17), 4106–4109 (2015).
18. H. T. Hattori, C. Seassal, E. Touraille, P. Rojo-Romeo, X. Letartre, G. Hollinger, P. Viktorovitch, L. Di Cioccio, M. Zussy, L. El Melhaoui, and J. M. Fedeli, "Heterogeneous integration of microdisk lasers on silicon strip waveguides for optical interconnects," *IEEE Photon. Technol. Lett.* **18**(1), 223–225 (2006).
19. H. Yoshioka, T. Ota, C. Chen, S. Ryu, K. Yasui, and Y. Oki, "Extreme ultralow lasing threshold of full polymeric fundamental microdisk printed with room temperature atmospheric ink-jet technique," *Sci. Rep.* **5**(1), 10623 (2015).
20. R. J. McMahon, *Avidin-Biotin Interaction Methods and Applications* (Humana Press 2008).
21. Y. Y. Lu, T. F. Shi, L. J. An, and Z.-G. Wang, "Intrinsic viscosity of polymers: From linear chains to dendrimers," *EPL* **97**(6), 64003 (2012).
22. P. Calvert, "Inkjet printing for materials and devices," *Chem. Mater.* **13**(10), 3299–3305 (2001).
23. K. T. A. Nasir, C. Chen, Y. Mikami, T. Takagishi, H. Yoshioka, M. Matsuyama, N. Nishimura, N. J. Vasa, and Y. Oki, "Lasing characteristics of a pyrromethene597-doped microdisk laser fabricated by the ink-jet printing method," *Jpn. J. Appl. Phys.* **58**(S1), S11C05 (2019).
24. Y. Mouhamad, P. M. Tabari, N. Clarke, R. A. L. Jones, and M. Geoghegan, "Dynamics of polymer film formation during spin coating," *J. Appl. Phys.* **116**(12), 123513 (2014).
25. N. J. deMol and M. J. E. Fischer, *Surface Plasmon Resonance Methods and Protocols* (Humana Press 2010).
26. G. E. Perlmann and L. G. Longworth, "The specific refractive increment of some purified proteins," *J. Am. Chem. Soc.* **70**(8), 2719–2724 (1948).
27. N. M. Kovalchuk, A. Trybala, V. Starov, O. Matar, and N. Ivanova, "Fluoro vs hydrocarbon surfactants: why do they differ in wetting performance?" *Adv. Colloid Interface Sci.* **210**, 65–71 (2014).
28. M. Miyasaka, N. Koike, Y. Fujiwara, H. Kudo, and T. Nishikubo, "Synthesis of hyperbranched fluorinated polymers with controllable refractive indices," *Polym. J.* **43**(3), 325–329 (2011).
29. D. Gandolfi, F. Ramiro-Manzano, F. J. Aparicio Rebollo, M. Ghulinyan, G. Pucker, and L. Pavesi, "Role of edge inclination in an optical microdisk resonator for label-free sensing," *Sensors* **15**(3), 4796–4809 (2015).
30. J. Voros, "The density and refractive index of adsorbing protein layers," *Biophys. J.* **87**(1), 553–561 (2004).
31. M. Oxborrow, "How to simulate the whispering-gallery modes of dielectric microresonators in FEMLAB/COMSOL," *Proc. SPIE* **6452**, 64520J (2007).
32. R. Yatabe, T. Onodera, and K. Toko, "Fabrication of an SPR sensor surface with antifouling properties for highly sensitive detection of 2,4,6-trinitrotoluene using surface-initiated atom transfer polymerization," *Sensors* **13**(7), 9294–9304 (2013).
33. M. Erol, H. Du, and S. Sukhishvili, "Control of specific attachment of proteins by adsorption of polymer layers," *Langmuir* **22**(26), 11329–11336 (2006).
34. R. Yatabe, O. Takeshi, and T. Kiyoshi, "Fabrication of surface plasmon resonance sensor surface with control of the non-specific adsorption and affinity for the detection of 2,4,6-trinitrotoluene using an antifouling copolymer," *Front. Bioeng. Biotechnol.* **2**, 10 (2014).
35. Y. L. Jeyachandran, J. A. Mielczarski, E. Mielczarski, and B. Rai, "Efficiency of blocking of non-specific interaction of different proteins by BSA adsorbed on hydrophobic and hydrophilic surfaces," *J. Colloid Interface Sci.* **341**(1), 136–142 (2010).